

## Introduction

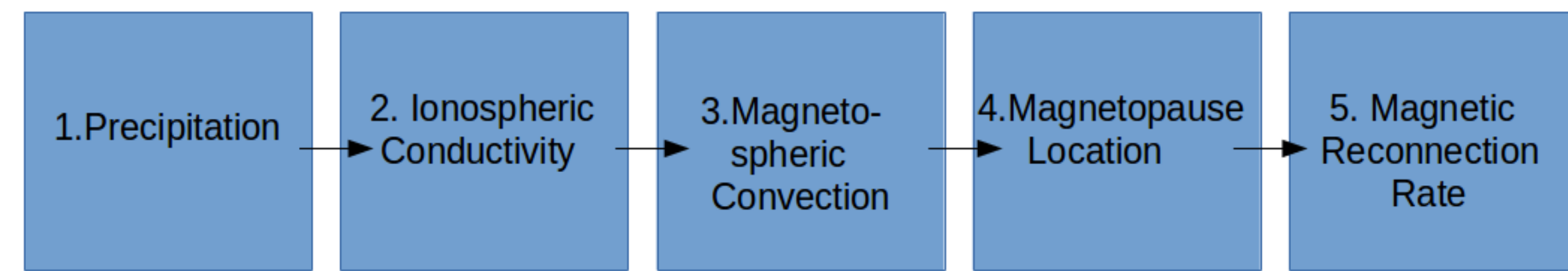


Figure 1: proposed cause and effect chain.

The Solar wind-magnetosphere-ionosphere-thermosphere (SMIT) system is highly coupled and there are many interconnections that affect every aspect of the SMIT system. This poster attempts to illustrate one of these connections in the SMIT system, figure 1 shows the proposed connection. There are many other effects contributing to each of these steps that in turn affects other parts of the magnetosphere, but for simplicity, figure 1 shows only the parts that are discussed in this poster.

To elucidate the role of particle precipitation the March 17, 2013 storm has been studied using the OpenGGCM-CTIM-RCM with three different simulations. We multiply the precipitation in each simulation by a precipitation factor (PF) of .01, 1, and 10. Different aspects of the magnetosphere for all three simulations are studied. Solar wind data from the ACE satellite for the March 17, 2013 storm is shown in figure 2. There is a large CME impact at about 5:30 UT.

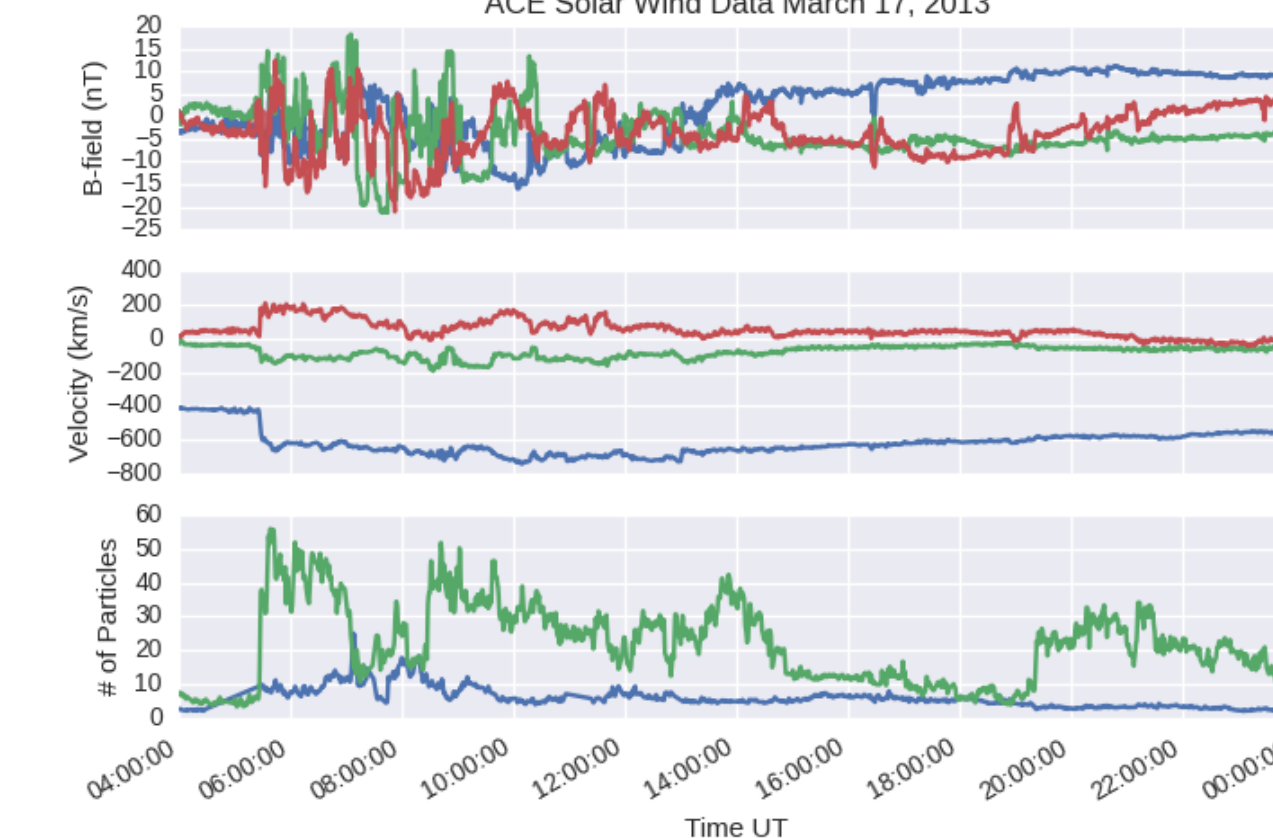


Figure 2: Solar wind parameters taken from the ACE satellite for March 17, 2013

## Particle Precipitation

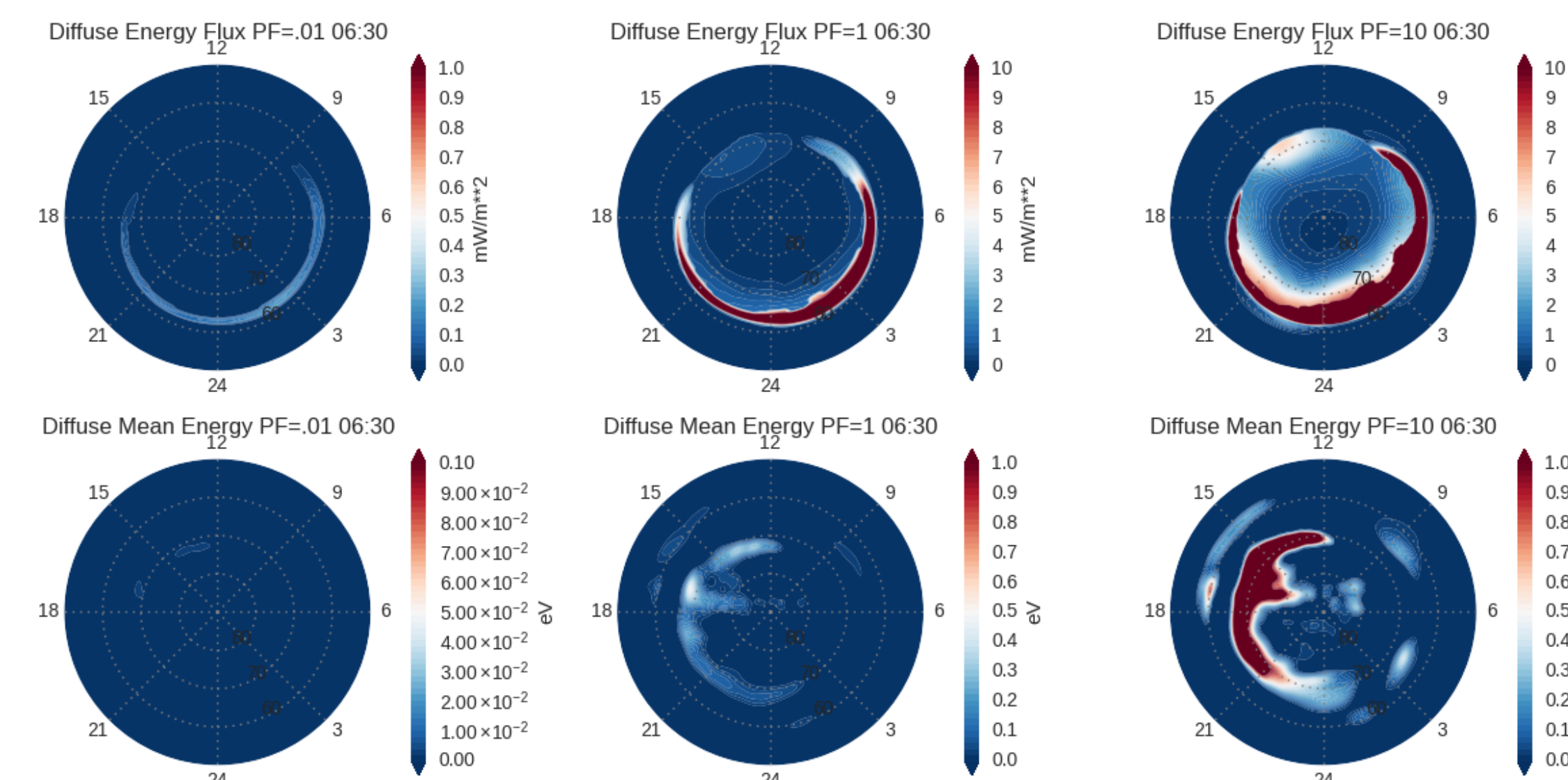


Figure 3: Particle precipitation for the northern hemisphere. Diffuse energy flux is shown on the top panels, with diffuse mean energy on the bottom panel, PF=.01, 1 and 10 are left, center, and right respectively.

The Knight calculation is used to find the precipitation from the MHD portion of the model. This results in the number of electrons and the mean energy of the electrons that precipitate for given conditions of potential and field aligned currents. With this information CTIM calculates the ionization and conductivities. Figure 3 shows the precipitation for the three PF's.

## Conductivity

The conductivity in the ionosphere has many important factors contributing to it, and precipitation makes a significant contribution as can be seen in figure 4. For the PF=.01 (left) case the dayside photoionization dominates the conductivity contribution, but for the PF=1 (center) case the precipitation conductivity is comparable in the auroral oval. In the PF=10 (right) case conductivity due to precipitation totally dominates.

Figure 4: The conductivity for the northern hemisphere at 6:30 UT, just after the impact of the ICME. Pederson conductivity is on the top panel, Hall conductivity on the bottom with PF=.01, 1, and 10 are shown left, center, and right respectively.

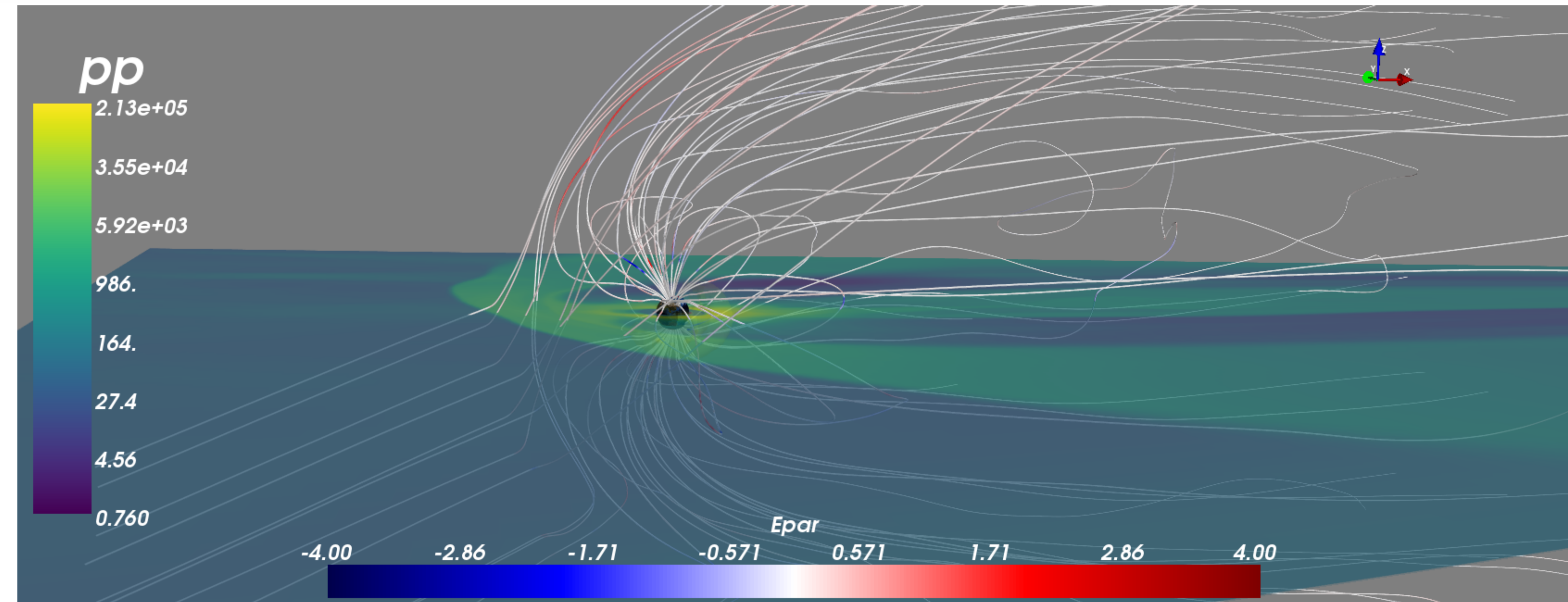
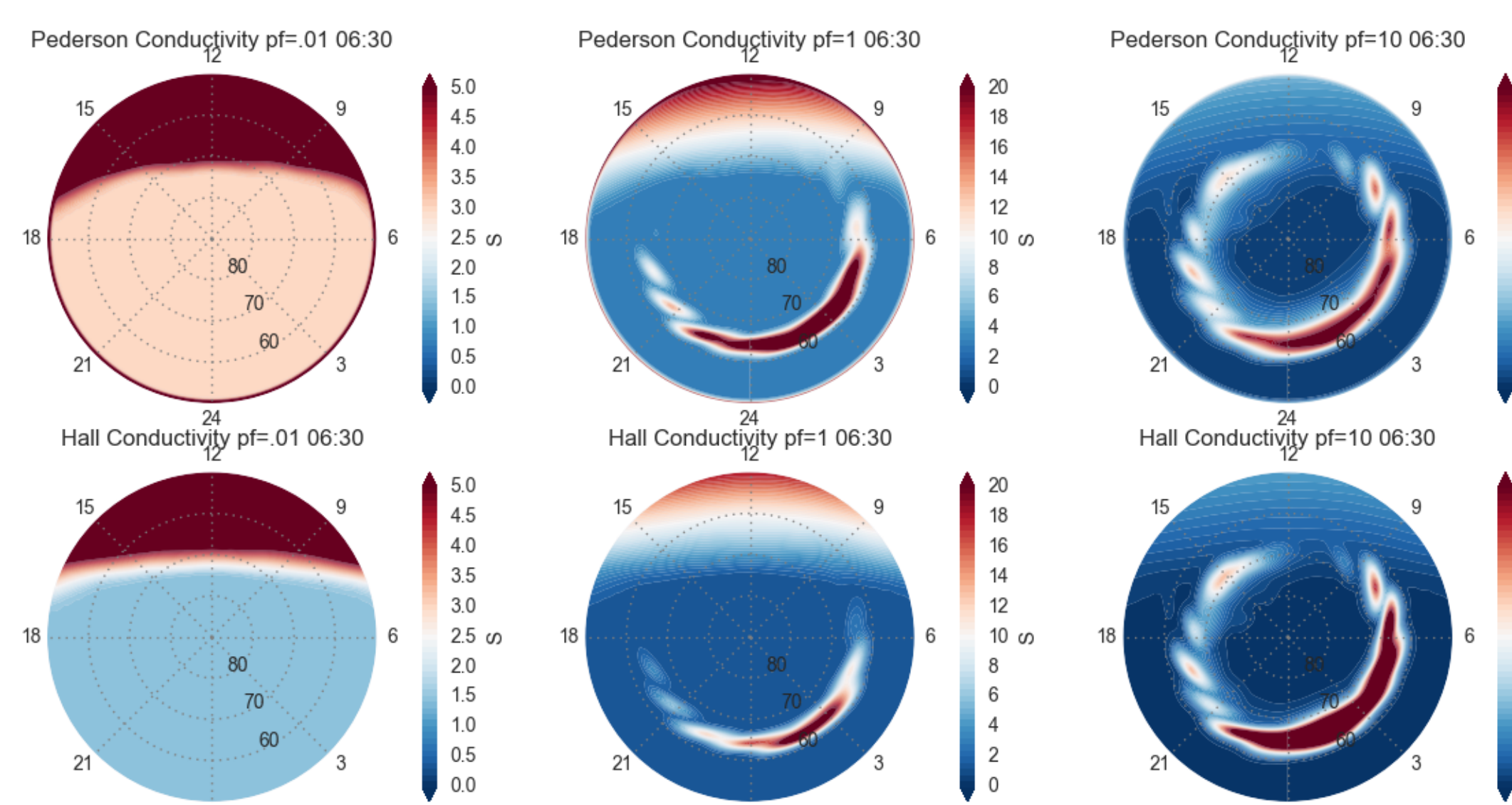


Figure 8: Depicts the earth's magnetosphere. The plasma pressure (pp) is shown in the x-y plane, the bowshock can be clearly seen. The lines emanating from the earth represent the magnetic field and the coloring of the lines shows the E parallel (Epar) along the magnetic field lines.

## Cross Polar Cap Potential

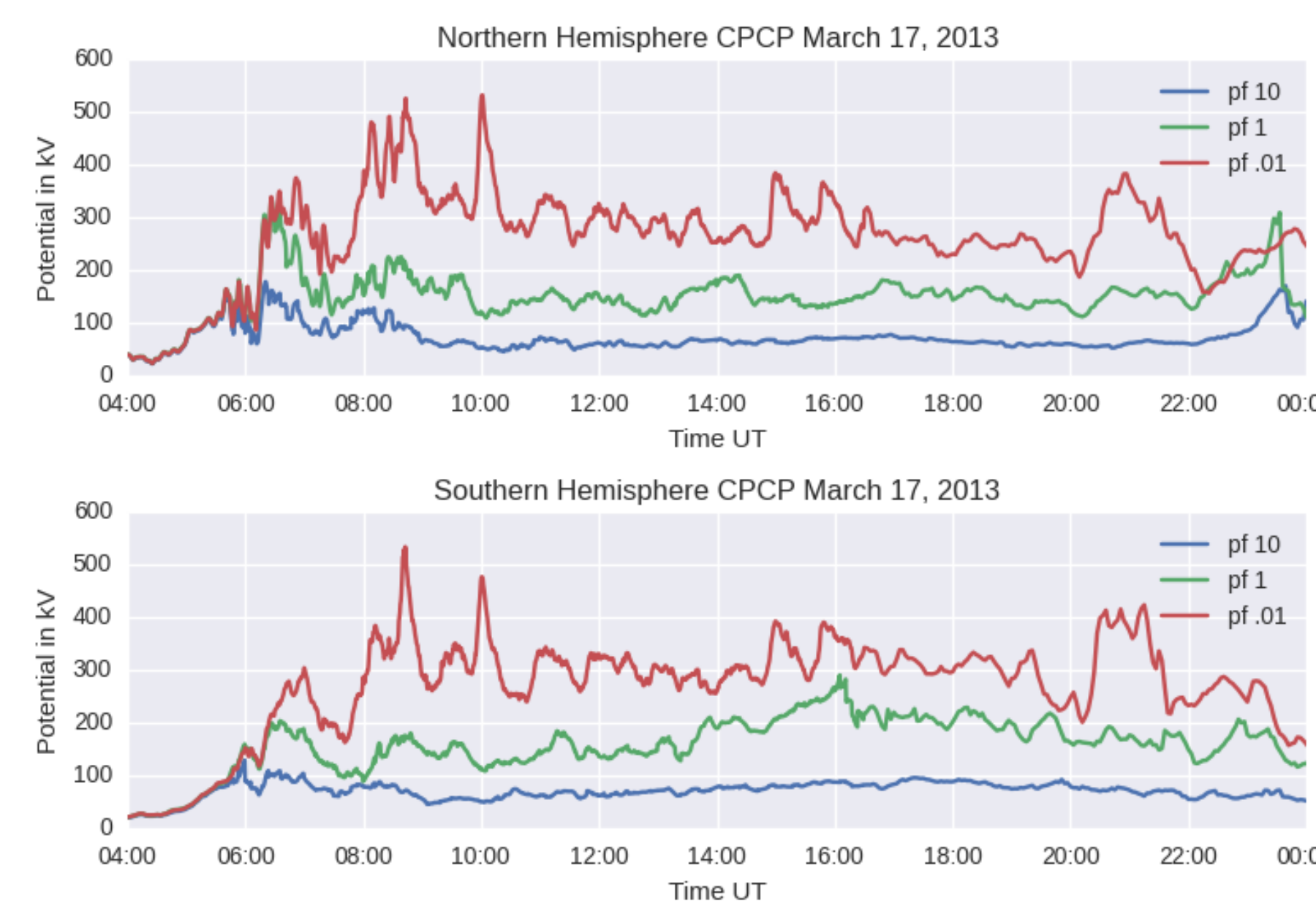


Figure 5: Cross polar cap potential for northern (top) and southern (bottom) hemisphere. All three PF simulations are shown.

The cross polar cap potential (CPCP) was modeled by finding the maximum and minimum potential for both the northern and southern hemispheres and the difference is the CPCP. In figure 5 there is a clear trend between precipitation and CPCP. The lower the precipitation (and conductivity) the higher the CPCP. Often CPCP can be understood as a measure of the flux through the magnetosphere and can give some indication of the reconnection.

## Magnetopause location

The dayside magnetopause location was studied to ascertain the effect of particle precipitation. Figure 6 shows the location of the magnetopause on the sun earth line. For the PF=.01 case the location has moved away from earth, with the PF=10 case closest to the earth. Increased ionospheric conductivity leads to magnetospheric convection being suppressed, resulting in a contracted magnetosphere which brings the dayside magnetopause location earthward.

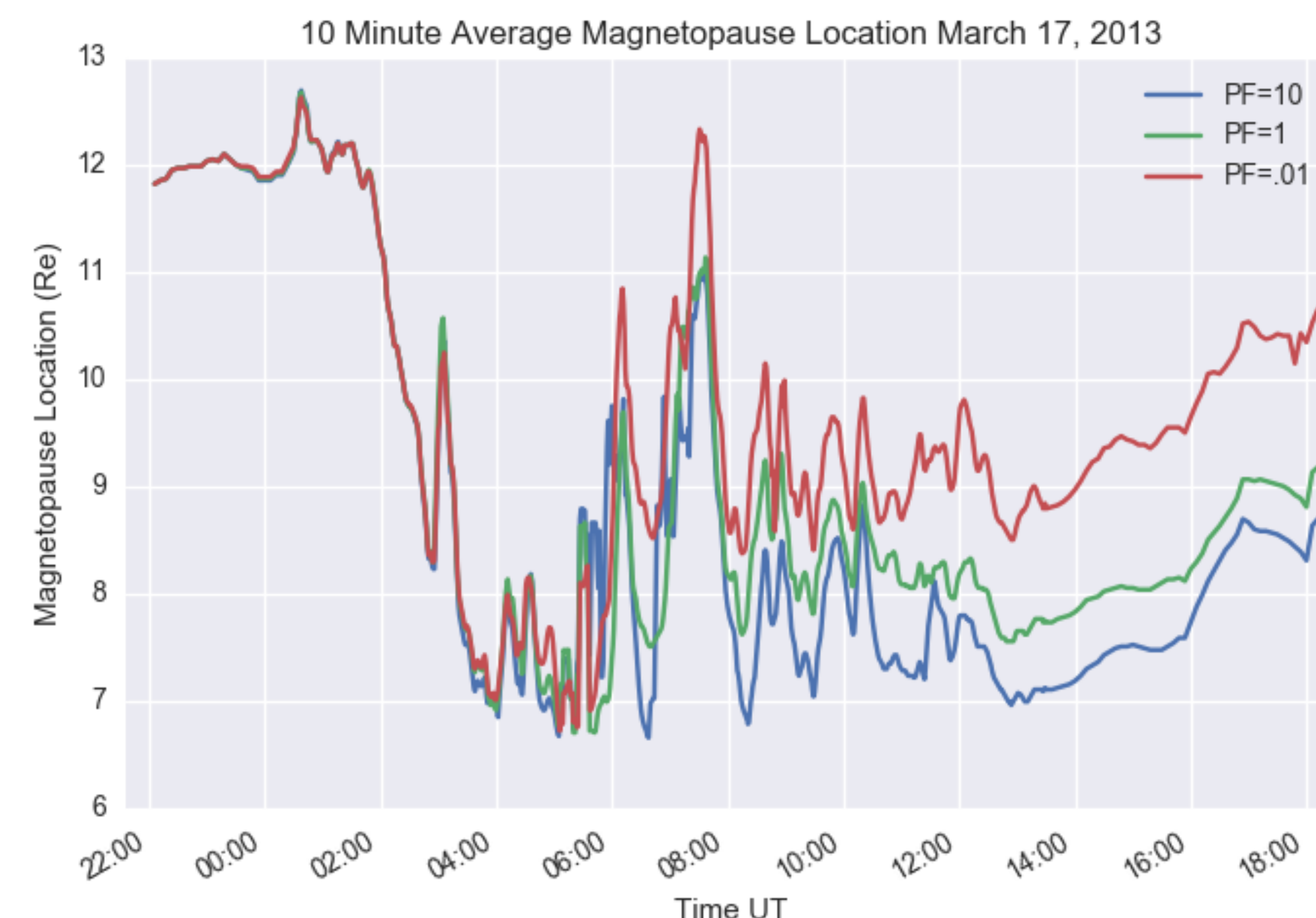


Figure 6: The ten minute averaged magnetopause location graphed for all three PF simulations for March 17, 2013. The location changes on time scales of seconds to minutes, but the ten minute average gives the general trend.

## Reconnection

To calculate the magnetic reconnection the Hesse et al [2005] method was implemented. This method integrates the parallel electric field over all magnetic field lines. Preliminary results of the reconnection rates are found in Figure 7 for both the northern and southern hemisphere. Most of the parameters looked at have had distinct differences for the duration of the simulation between the different PF cases, the reconnection is more difficult to see a clear difference for the entire duration. At the maximum spread, about 18:00 hours, there is a difference of up to 40%, but as can be seen it is not a simple linear increase for the duration of the simulation.

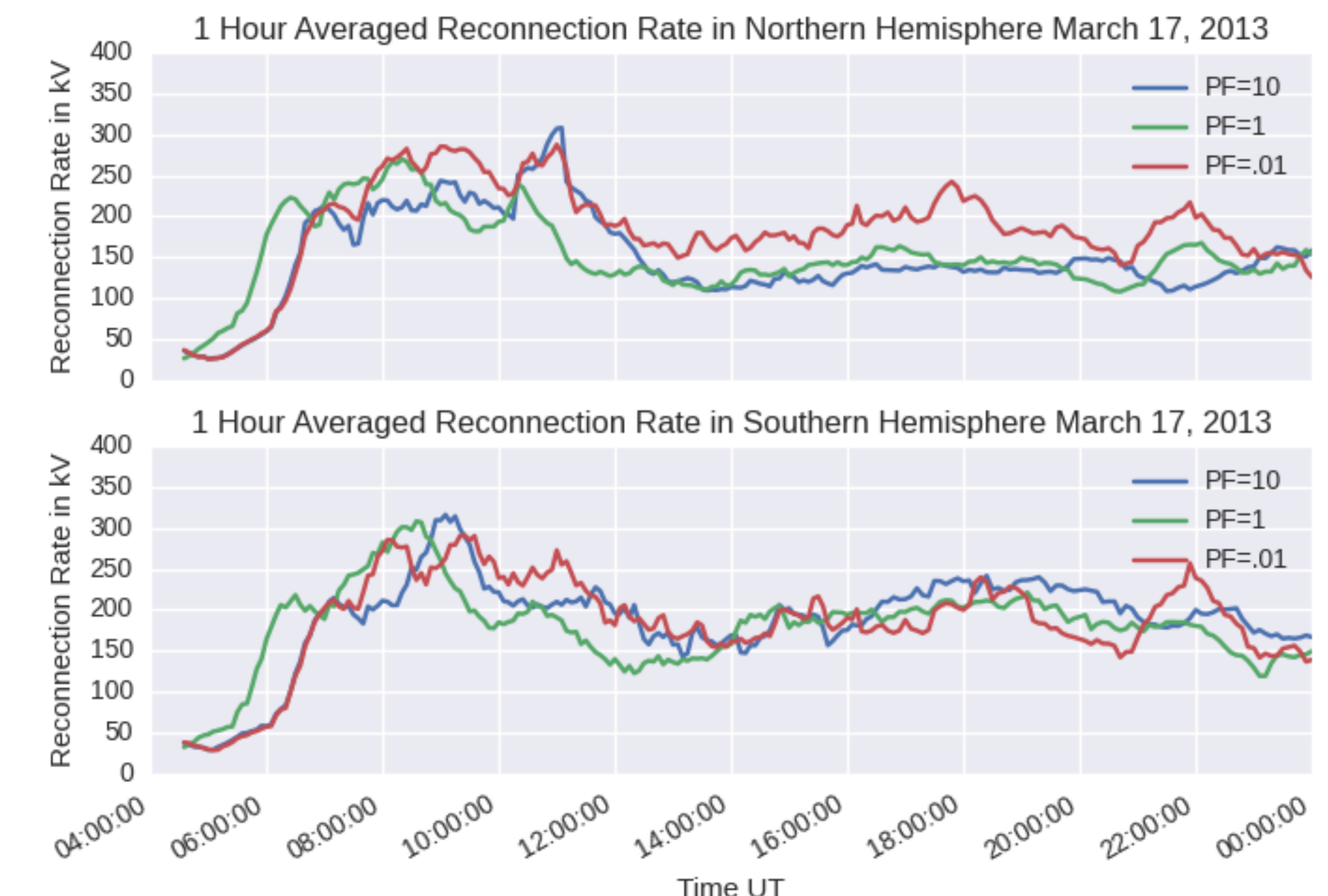


Figure 7: Magnetic reconnection rate for the northern hemisphere (top) and southern hemisphere (bottom). Each of the PF cases are graphed for each case.

## Conclusions

Changing the precipitation has wide ranging effects in the SMIT system and even affects things like dayside magnetopause reconnection. The change in magnetic reconnection due to precipitation is not a simple linear relation, but involves interesting dynamics that highlight the complex and interconnected nature of the SMIT system.

## References and Acknowledgments

- Hesse, M., T. G. Forbes, and J. Birn (2005), On the Relation between Reconnected Magnetic Flux and Parallel Electric Fields in the Solar Corona, *Astrophys. J.*, 631(2), 1227-1238, doi:10.1086/432677.

The author is grateful for the student travel support received from CEDAR.